Tethys, 4, 33–43, 2007
www.tethys.cat
ISSN-1697-1523
eISSN-1139-3394
DOI:10.3369/tethys.2007.4.05

Journal edited by **ACAM**
(Associació Catalana de Meteorologia)

A study of three well-defined temporal intervals in a stably stratified night

M. Vich, M. A. Jiménez and J. Cuxart

Meteorology group, Physics department, Universitat de les Illes Balears. Cra. Valldemossa, km. 7.5, 07122, Palma de Mallorca

Received: 12-VI-2007 – Accepted: 7-XII-2007 – **Translated version**

Correspondence to: mar.vich@uib.es

Abstract

A stable stratified night during the experimental SABLES-98 campaign was studied. It was found that the night could be divided into three distinct parts: an initial phase of transition, with significant changes in all the variables until a quasi-steady regime was reached; a second part dominated by the surface radiative cooling; and a final stage that revealed no significant changes. Each of these intervals was studied separately through the analysis of the vertical profiles, turbulence, spectra and the probability density functions.

1 Introduction

The Atmospheric Boundary Layer (ABL) is the part of the troposphere that is directly influenced by the presence of the Earth's surface in relatively short time scales (of about one hour). The factors that regulate this influence are both thermal (surface warming or cooling) and dynamic, due to the interaction between wind and surface. Throughout the day usually both factors produce turbulent mixing, while during the night stable thermal stratification inhibits the dynamic production of turbulence generated by wind shear. On calm nights with almost no wind of synoptic or mesoscalar origin surface radiative cooling can be significant. The absence of general wind configures a regime with no sustained turbulence, significant vertical gradients of the meteorological variables or establishment of local circulations due to surface thermal differences.

This regime is commonly known as the Stably Stratified Boundary Layer (SBL) and is difficult to characterize. Characterization is hard due to the predominance of local effects. Moreover, observations show that the SBL has no stationary behavior, but it has certain patterns depending on the time of the night (Cuxart et al., 2007). In the present study a readjustment period was reported at the beginning of the night during the changing of regimes from day to night. Local circulations at low height were commonly established during this phase. Such circulations are marked by wind maxima that usually correspond to katabatic flows. A quasi-steady regime was established at a later stage with a strong surface cooling, which often ended with an intense and short mixing episode. Following this mixing episode was an evolution characterized by changes in temperature and wind of a lesser magnitude without a marked tendency.

We cannot justify this pattern because our assumptions are based on indirect evidence or numeric simulations, however, we can characterize evolutions by analyzing the available data.

In this study we analyzed a night during the SABLES-98 campaign (Stable Atmospheric Boundary Layer Experiment in Spain), which is briefly described in section two. The characteristics of each interval during the night were analyzed and are described in the following sections. Some conclusions and orientation guides for future research on this topic are offered.

2 Experimental data and data processing

The experimental SABLES-98 campaign took place at the CIBA (Spanish acronym for research center in low atmosphere), near Valladolid, September 10 - 28, 1998. The main objective was to evaluate the phenomena that occur in mid-latitude SBL. Among other instruments, two meteorological masts were used (of 100 m and 10 m height), which were equipped with five sonic anemometers and fifteen thermocouples. A sodar system was also used, as well as a tethered balloon, which was launched during the central days of the campaign under the appropriate meteorological condi-

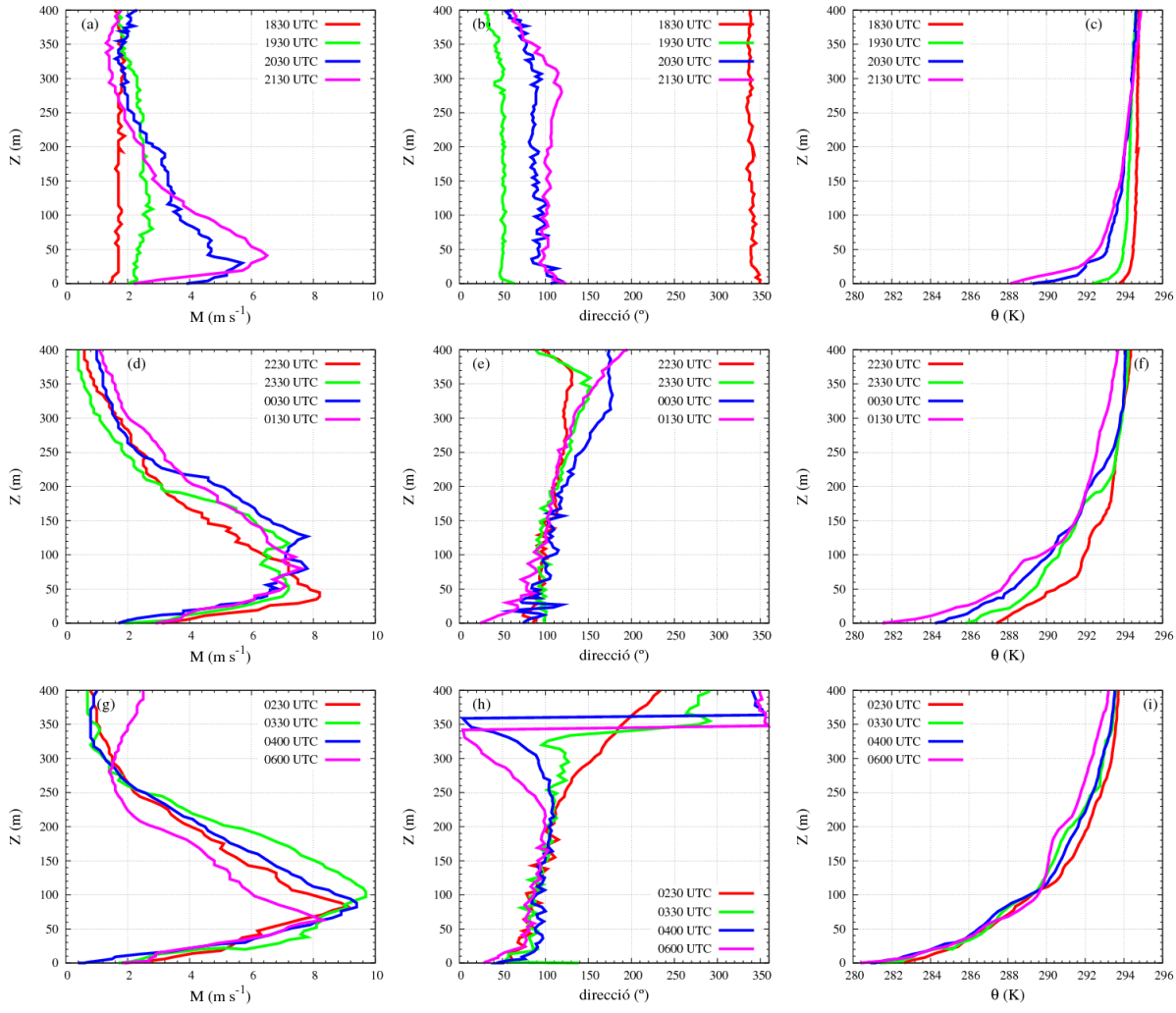

Figure 1. Soundings of the night of September 15 - 16, 1998, measured during the SABLES-98 campaign. Profiles are separated in intervals, as described in the text. **INTERVAL 1**: (a) wind speed (b) direction and (c) potential temperature. The same for **INTERVAL 2** in (d), (e) and (f) and for **INTERVAL 3** in (g), (h) and (i).

tions. Details of the instruments used during SABLES-98 and the description of the observed phenomena are reported in Cuxart et al. (2000).

During the first days of SABLES-98 (September 10 - 13), there were strong winds and the conditions were suitable for studying neutral and weakly stable boundary layers sheared by the wind. During the following week (September 14 - 21), conditions were favorable to measure SBL. In the final days of SABLES-98 (September 22 - 28), CIBA was influenced by a low-pressure system and some clouds appeared, with rainfall in the final days.

Some nights in SABLES-98 were more intensely analyzed than others due to more favorable conditions for taking measurements such as the nights between September 14 - 21. This period was defined by an anticyclonic and stationary situation with a weak surface pressure gradient, which allowed the development of local effects. During the night winds came from the NE and conditions were stable. This intensive analysis allowed us to characterize the phenomena found in the results (Cuxart et al., 2000; Yagüe et al., 2006, Conangla et al., 2008) using one-dimensional simulations (Conangla and Cuxart, 2006) and Large Eddy Simulations (LES) (Jiménez and Cuxart, 2005; Cuxart and Jiménez, 2007). Mesoscale simulations were recently carried out to investigate the configuration of the flows in the basin where the CIBA is located, which is similar to previous studies carried out in Mallorca (Cuxart et al., 2007).

The night data obtained in September 15 - 16 still have not been analyzed in detail. This seems to be an archetypical CIBA night. Consistent with the other days of the week, the synoptic situation was characterized by a weak pressure gradient and an E component wind. This easterly wind was due to an anticyclone with its center over the Atlantic Ocean at the NW of the Iberian Peninsula. In order to analyze this night in more detail, we will use data obtained from the 100 m mast, soundings from the tethered balloon (12 during the

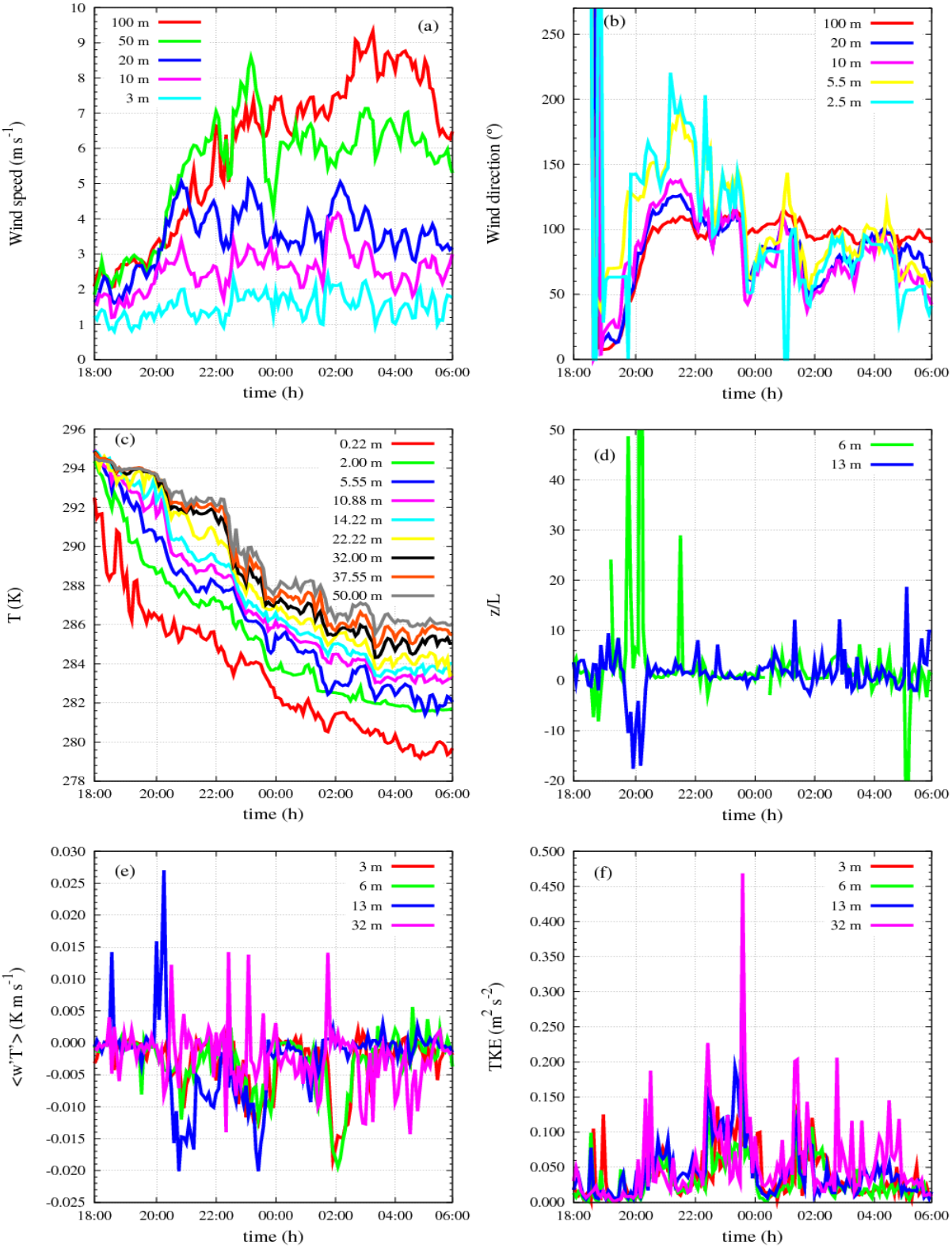

Figure 2. Temporal series (5-min means) of the data measured by the 100 m and 10 m masts, from 18:00 UTC on September 15 to 06:00 UTC September 16 1998; (a) and (b) wind and direction module, respectively, (c) temperature, (d) stability parameter, z/L, where z is height and L is the Monin-Obukhov length, (e) vertical temperature flux and (f) turbulent kinetic energy, $TKE = 0.5(\overline{u'^2} + \overline{v'^2} + \overline{w'^2})$, where $\overline{u'^2}$, $\overline{v'^2}$ and $\overline{w'^2}$ are the variations in the three directions of the wind.

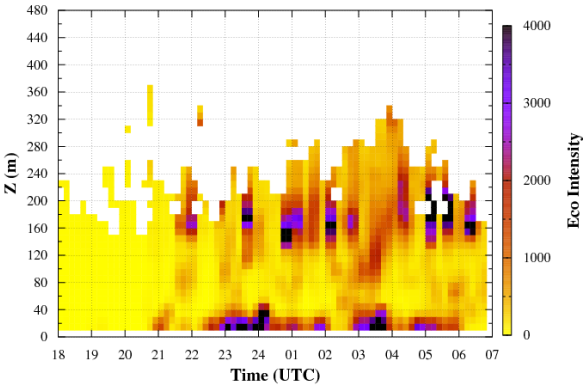

Figure 3. The echoes measured by the sodar during the night of September 15 - 16, 1998.

night), and sodar echoes. As well as classical profile analyses, we will use probability density functions (PDF) to calculate statistics from data without the need of a high time resolution. Furthermore probability density functions have no associated conceptual problems when defining averaging time because a spectral gap is not necessary (Monin and Yaglom, 1971). To finalize the analysis a series of fluxes will be inspected, calculated in the classical way. Spectra of some of the selected variables will also be inspected. In this case, the fluxes are calculated based on five- minute averages (spectra show minimum spectral intensity around this period), using high frequency data extracted from the SABLES-98 database and the Reynolds averaging method, taking the direction of the mean wind as x.

PDFs can be calculated from any data set. In this paper they are calculated from measurements taken by sonic anemometers (a time series of the whole night) for wind and virtual temperature (from now on virtual temperature will be referred to as temperature). The corresponding PDF for a data set is $B(x)$; it represents the probability of finding an x value between x and $x \pm \Delta x$, where Δx is the PDF discretization interval. The PDF value is normalized to one ($\int_{-\infty}^{\infty} B(x)dx = 1$) and is usually represented graphically as $\sigma_x B(x')$ where $x' = \frac{x-\overline{x}}{\sigma_x}$ where $\overline{x}$ is the average value and σ_x is the standard deviation. However, to effectively study the behavior in the extremes (which correspond to phenomena away from the average value and rather unlikely), the scale of the y axis is logarithmically chosen. A more detailed description of the PDFs calculation can be found in Tennekes and Lumley (1982).

PDFs have been used in the past to analyze laboratory experiments, experimental measurements and LES simulations. Examples of this include a study by Deardorff and Willis (1985), in which the laboratory measurements of a water tank were analyzed, or Mahrt and Paumier (1984), during a study of the cloudy boundary layer. More recently, Jiménez and Cuxart (2006) analyzed the LES of the SBL using this method. Chu et al. (1996) also used PDFs to analyze observations of the boundary layer, however, they used a shorter time period than the one used in this study (fifteen-minute time sequences compared to twelve-hour time series, which is the whole night).

3 General characteristics of nighttime

During the night period of September 15 - 16, there was a local maximum of wind in the low layers -Low-Level Jet, LLJ- early in the night (from 20:00 UTC). Apart from some episodes of sporadic mixing, which temporary altered its characteristics, the LLJ was almost constant throughout the night. A similar situation occurred on the night of September 20; although in this case the LLJ appeared at a later stage when night conditions were fully developed (from 00:00 UTC). This LLJ was steady only until 02:30 UTC, at which point a strong mixing occurred.

Figure 1 shows the evolution of the wind speed, direction, and temperature, measured by the soundings of the tethered balloons during the night. The night was divided into three different intervals; in the first interval (soundings from 18:30 to 21:30 UTC, **INTERVAL 1**) the wind turns clockwise from the north-northwest to the east at a rate double that of an inertial oscillation from the well-mixed value of the end of the day. Wind is constant over 250 meters above ground level and increases in speed in the lower layers. This increase in speed is in principle because of the inertial oscillation, which is highest over the SBL. It then slows down due to turbulence close to the ground. The temperature near the ground becomes progressively colder. We consider this interval over when the direction of the wind stops its evolution.

The second interval (soundings from 22:30 to 01:30 UTC, **INTERVAL 2**) has a constant wind direction with time from the east. An LLJ is established with wind maxima of 8 m s^{-1}, which is localized between 50 and 120 m. Below 200 m the temperature decreases at a fast rate (up to 1.5 K h^{-1} for 2 m height) throughout the whole layer, which contrasts with the static appearance of the wind.

The last interval (soundings from 02:30 to 06:00 UTC, **INTERVAL 3**) was characterized differently. There was a complete stop in the column cooling process, with no significant changes in the wind direction. There was a tendency of the maximum wind to rise up and become stronger, except at the end of the night when it became weaker.

The time series obtained by the mast sensors confirm this evolution (Figure 2), and illustrate the time variability between soundings. From Figure 2 it is clear that wind direction oscillates during a period of about two hours below 100 m and that wind speed, varies at forty minute intervals. These variations are similar to those described for temperature. Turbulent variables reveal episodes of intermittent turbulence (which are easy to see in turbulent

kinetic energy -TKE-) and changes in the sign of the heat flux. The results also demonstrate that turbulence is often more intense in the upper levels than in the lower ones.

Figure 3 shows the sodar echoes during the night, which indicate the presence of reflecting structures near the ground (below 50 m) and on the upper side of the jet (near 150 m). Thus we can assume these two areas to be turbulent. An episode of echoes (turbulence) in the entire column at 03:30 UTC is coincides with the beginning of the third defined interval.

4 Analysis of intervals

4.1 Establishment of the LLJ

As it has already been described, wind turns clockwise from sunset until it becomes eastern. The air near the surface becomes colder and an LLJ is generated from 20:30 UTC onwards. Potential temperature shows two distinct gradients: a strong one near the ground and a weaker one above until the height of the wind maximum. There is a strong turbulence episode between 20:00 and 20:30 UTC, which coincides with the establishment of the LLJ. It could also be related to considerable thermal decoupling. This occurs between the layers over the surface and air at heights above 10 m ($(T_{10m} - T_{0.22m}) = 7$ K just before the turbulent episode at 20:00 UTC and later at 20:30 UTC ($T_{10m} - T_{0.22m}) = 4$ K). The LLJ probably originates from an inertial oscillation (even if the period is shorter due to reasons still unexplained). The moment when its direction becomes fixed is probably related to a basin flow (katabatic or mesoscalar) that is nearly consistent in direction during the rest of the night (Cuxart, 2008).

The stability parameter is z/L, where z is height and $L = -\frac{\overline{\theta_v} {u_*}^3}{kg\overline{w'\theta'}}$ is the Monin-Obukhov length, with ${u_*}^2 = (\overline{u'w'}^2 + \overline{u'w'}^2)^{0.5}$ as the friction speed, calculated from moment fluxes on the surface (collected at 6 m). As described by Mahrt et al. (1998), parameter z/L, calculated approximately at a height of 10 m, indicates that state if the conditions are weakly stable ($z/L < 0.1$), strongly stable ($z/L > 1$) or transition (intermediate). Figure 2d shows the time series of this parameter calculated at two levels: 6 m and 13 m, some there are no turbulence measurements at 10 m. It appears that in this night interval $z/L \approx 1$, which indicates that the regime is strongly stable and in some instants $z/L >> 1$. By contrast, in the calculation at 13 m there are some instants when z/L is negative, which indicates periods of instability. This is consistent with the time series of $<w'\theta'>$, which takes high positive values at this level. The events of higher instability on this level happen to be around 20:30 UTC, where there is a well-mixed layer over the cooling superficial inversion. This can be seen in the sounding and in the temperature time series.

Figure 4a illustrates the evolution of the bulk Richardson number, calculated between different measurement levels as $Ri_B = -\frac{g\Delta\overline{\theta_v}\Delta z}{\overline{\theta_v}(\Delta\overline{U})^2+(\Delta\overline{V})^2}$. For this interval, consistent with what has recently been described, values are higher than the critical values (0.25 or 1 depending on the calculation method) near the surface and appear stable. However, they become negative over the cooling inversion, indicating the possibility of turbulence on these levels.

PDFs are shown in Figures 5a and 5b. As it is an adjustment period, it cannot be considered in equilibrium. The PDF of the temperature (Figure 5a) fluctuates a lot as it cools at every level but this cooling is not constant. For instance, at 20:30 UTC there is a sudden cooling (Figure 2c), mainly above 10 m, which makes the entire superior column instable. As a result of this, the PDF corresponding to this interval has many peaks around the average value, while the PDF at 6 m does not fluctuate as much because the cooling rate is more regular. The PDF of the wind (Figure 5b) at 6 m is bimodal with two similar probability peaks with values fluctuating around the average. On higher levels, however, the shape is close to Gaussian. The most probable values are lower than the average but the higher fluctuations are much higher than the average value. These fluctuations are further from the average than the lower values. This behavior is correlated with the evolution of the wind on these levels (Figure 2a). Wind fluctuates near the ground (3 m) and its speed tends to increase at higher levels.

Energy spectra (calculated from $E = \frac{1}{2}(u^2 + v^2 + w^2)$) are shown in Figure 6 for each of the intervals. They were calculated using FFT with a 14 width Kaiser-Bessel window over the series produced by the sonic at 20 Hz. A variable filter was applied to them therefore the higher frequencies were more damped than the lower ones.

In the strong surface cooling zone (at 6 m in Figure 6a) the spectrum appears to end with an increase of energy in the higher frequencies. This indicates that the structures that led to turbulent dissipation are too small to be properly resolved in this sampling frequency. For this reason the inertial subrange cannot be explicitly seen (-2/3 slope). An inertial subrange seems to exist over this area for structures with times equal to or under ten seconds, an energetic gap of about 100 s and traces of the buoyancy subrange (-2 slope), where quasi-bidimensional motions dominate (Stull, 1988).

4.2 Intense surface cooling

The sodar (Figure 3) shows the two areas where there is a strong echo between 21:30 and 02:30 UTC, near the ground and on the higher part of the jet, with some episodes of sporadic mixing. The intense surface cooling seems to cause a decoupling between the Surface Layer (SL) and the air above it, which experiences no significant turbulent friction. However, it seems that the flow is fed by a non-local factor, given the persistence in its direction. The surface cooling probably has a radiative origin and the transmission of such cooling to the top is done by turbulent mixing with a mechanic origin, which is more intense than in the first interval.

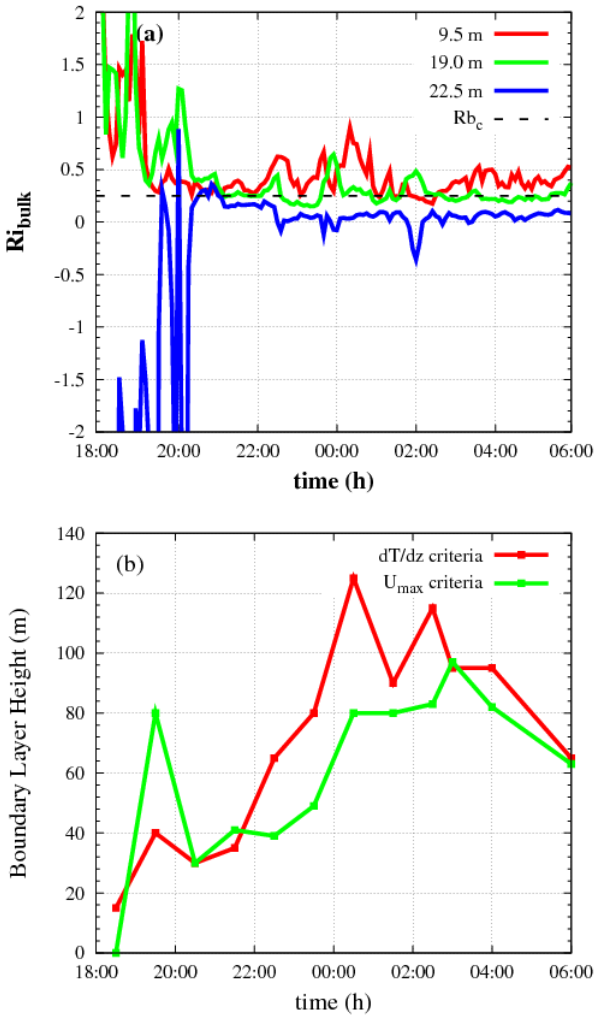

Figure 4. (a) Bulk Richardson number calculated from Ri_B (b) Height of the SBL, according to two different criteria (where the temperature gradient increases to its maximum and height of the wind is also at its maximum).

The height of the maximum temperature gradient no longer coincides with the LLJ maximum height (Figure 4b) (even if the wind maximum is often in the surface cooling area). Similar situations were observed during the CASES-99 campaign (the Cooperative Atmosphere-Surface Exchange Study-1999, CASES-99; Poulos et al., 2002) in the great plains of the United States, even when the LLJ was higher. In the LLJ over the Baltic Sea (Smedman et al., 1995), a strong surface inversion was also found, and the wind maximum of the LLJ was below the inversion (see Figure 5 in Smedman et al., 1995). The high turbulence revealed by the sodar is similar to the 1D model simulations (Conangla and Cuxart, 2006) and the LES model simulations (Cuxart and Jiménez, 2007).

Oscillations in the low layers of the wind direction remain unexplained. They could be attributed to gravity currents, but they could also be due to local decoupling which enlarges the shear in the direction and results in a mixing episode with the upper layer. Further research on direction variability of weak winds in the SL is needed.

Instability causes high values with changing sign in the heat flux and in the stability parameter. This is similar to those measured during some stable nights in CASES-99. Coulter and Doran (2002) found that surface temperature fluxes during nights in CASES-99 were ca. $<w\theta>$ = -0.010 K m s^{-1}, but in some instants could be much higher or lower. Measurements taken at different locations showed that those intermittences were not correlated but in fact strongly influenced by local effects (more details at Cuxart et al., 2002).

The stability parameter z/L shows how, in general, this interval is less stable than the previous one and experiences less sudden variations. Wind acceleration generates shear and causes the production of more TKE, which simultaneously destroys stability. According to the classification by Mahrt et al. (1998), this interval corresponds to a regime of stability between weak and strong ($0.1 < z/L < 1$). The bulk Richardson number (Figure 4b) shows that sustained stability is not strong, with values below the critical just over the surface cooling inversion.

The PDF of the temperature in this interval has different well defined maxima, which correspond to the background regime and to the different mixing episodes. Such behavior is similar on all three levels as this arrival of warm air from above (or raising cold air) can be noticed in the entire air column. However, they are slightly out of phase (see Figure 2c). The PDF of the wind (Figure 5d) at 6 m and 13 m is similar, with the values for maximum probability being below average. By contrast, the PDF at 32 m shows the opposite behavior (maximum probability values are above average). A possible explanation for this is that when an LLJ develops, the wind at 32 m tends to accelerate more than the wind near the ground (see Figures 1d and 2a).

The spectrum is similar to the one in the first interval but more energetic. With more turbulence the first level can also generate an inertial subrange on the first measurement level.

4.3 Stationarity

This interval maintains a well-formed LLJ that is slightly more intense at the height of maximum speed. The stronger shear may explain the high values for the heat flux and the TKE at 32 m, without clearly affecting the SL. The stationarity of the temperature profile is remarkable, although surface cooling continues, now in a more moderate rate (1K/4h). In this interval, the height of the LLJ maximum and the height of the maximum temperature gradient are relatively similar (Figure 4b). The coincidence in the heights of the LLJ maximum and temperature inversion may explain the absence of clear mixing episodes in the entire column (this is clear in the sodar record (Figura 3)), which acts as a barrier for matter and energy exchanges (see Cuxart and Jiménez,

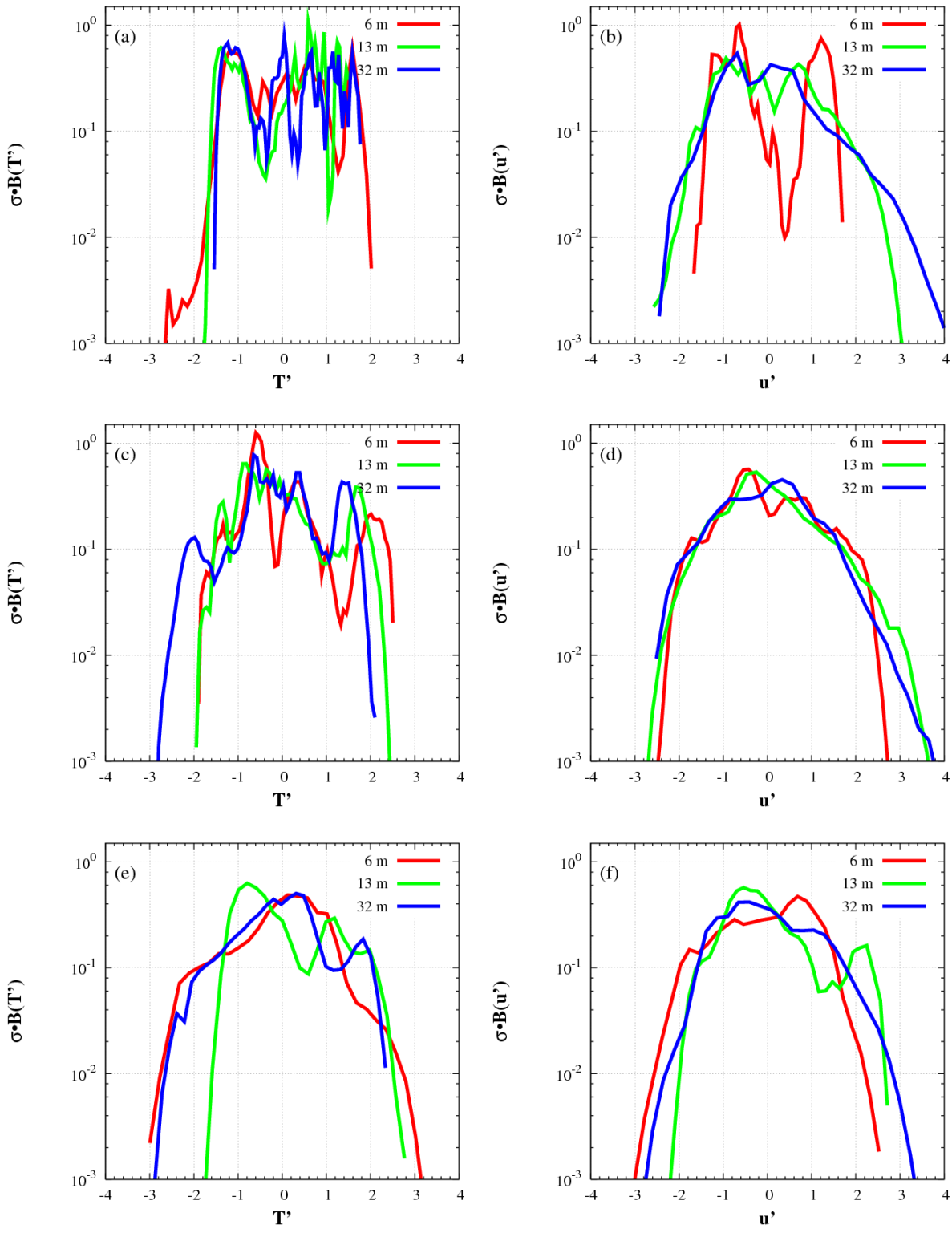

Figure 5. PDFs calculated for the intervals defined in the text. (a) and (b) are the PDFs of temperature and wind for **INTERVAL 1**, respectively; (c) and (d) are the same applied to **INTERVAL 2**; (e) and (f) are the same applied to **INTERVAL 3**. The PDFs were normalized by $T' = \frac{T-\overline{T}}{\sigma_T}$ and $u' = \frac{T-\overline{u}}{\sigma_u}$ where $\overline{T}$ and $\overline{u}$ are the average values and σ_T and σ_u are the standard deviations.

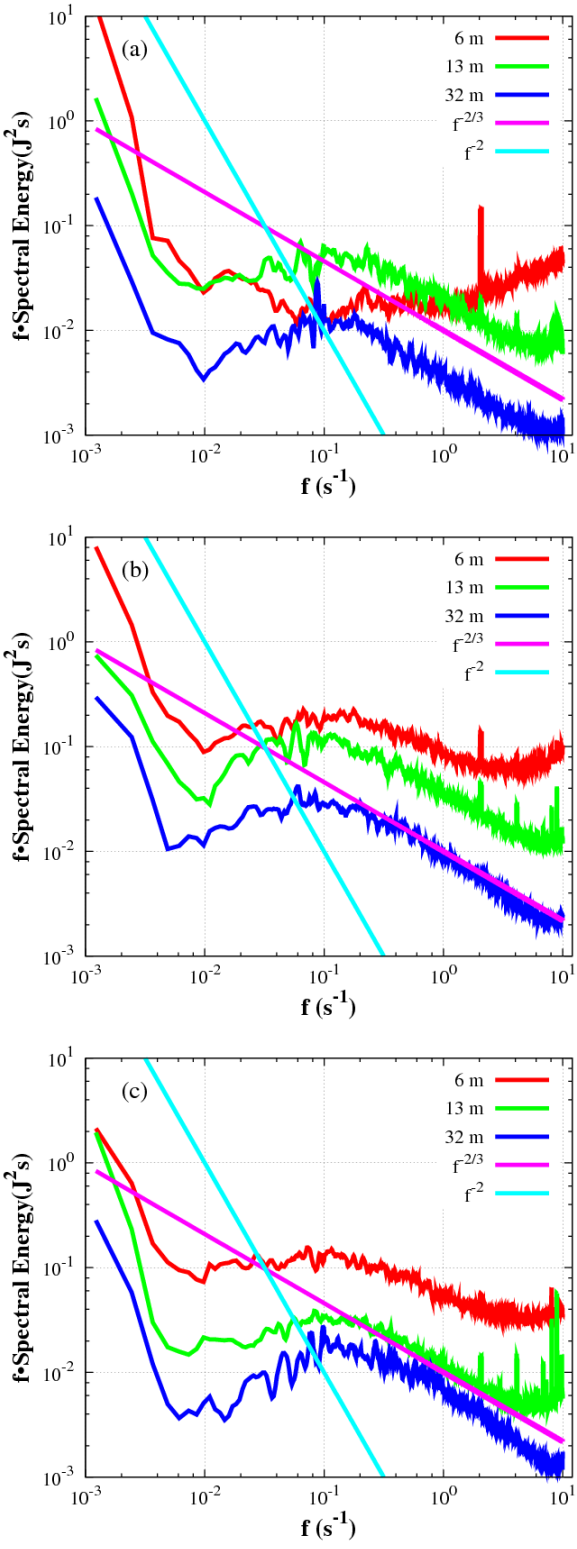

Figure 6. The spectrum of the energy calculated from $E = \frac{1}{2}(u^2 + v^2 + w^2)$ where u, v and w are the three wind components measured by the sonics. Inertial subrange slope ($f^{-2/3}$) and buoyancy subrange (f^{-2}). (a) **INTERVAL 1**, (b) **INTERVAL 2** i (c) **INTERVAL 3**.

2007). Below the jet, different layers in the temperature profile can be identified, which correspond to inversions at 50 m, 100 m and 200 m. This phenomenon is known as layering and was also observed during the nights at CASES-99 campaign (Poulos et al., 2002).

Temperature increases with height and maintains a stronger gradient under 10.88 m than above it. This explains how vertical motions are inhibited in this layer by the strong stratification stability and also by the presence of a stronger heat flux and TKE values above the layer. This is inconsistent with the theoretical expectations (Garratt, 1992) of a temperature profile which increases with height. Garratt in fact admits that his theory may be invalid in the SL, which is what is seen in this study.

The stationarity of the regime is reflected in the PDFs. Temperature PDFs (Figure 5e) have fewer peaks in their central part but are wider. Wind PDFs (Figure 5f) at 13 m and 32 m are similar, and the probability maximum is below the mean value. However, the opposite is found for wind PDFs at 6 m. This could be explained by the weakening of the LLJ as sunrise approaches. This effect is most noticeable close to the LLJ, whereas the wind near the surface has no significant variation. Spectra are very similar to those in the second interval; there is slight displacement of the spectral gap towards larger structures (of about 5 minutes) and some accumulation of spectral energy at 13 m, precisely at the higher limit of the temperature superficial inversion.

If the PDFs calculated for any of the intervals are compared with those from Chu et al. (1996), the PDFs in the later case are clearly more Gaussian. This also occurs when PDFs are calculated from LES simulations (Jiménez and Cuxart, 2006). The PDFs in this study, which are significantly out of Gaussianity, could be explained by the scales of motion present in the series and also from the lack of stationarity in the series (except in the final interval).

5 Comparison of intervals

A number of parameters are usually used to characterize the state of a turbulent regime. In this section we descriptively analyze a selection of parameters for the whole night. A possible definition of SBL is the layer where there is measurable turbulence over a definite threshold value (TKE over 0.001 $m^2 s^{-2}$ is usually taken). In this study, no profiles are available for this variable. However, Figure 2f illustrates that at each of the three levels with high frequency variables (6, 13 and 32 m) the TKE values are generally above this value. Figure 1f also shows that it is possible that the SBL extends to at least 32 m. The stability parameter z/L is positive throughout the whole night, indicating a stable stratification below 32 m except during a short period in the first interval, where z/L is very high (between 6 m and 13 m) which indicates decoupling between the layer near the ground and the ones above, unstably stratified.

The Richardson number is higher than the theoretical critical value for the layers near the ground (Figure 4a),

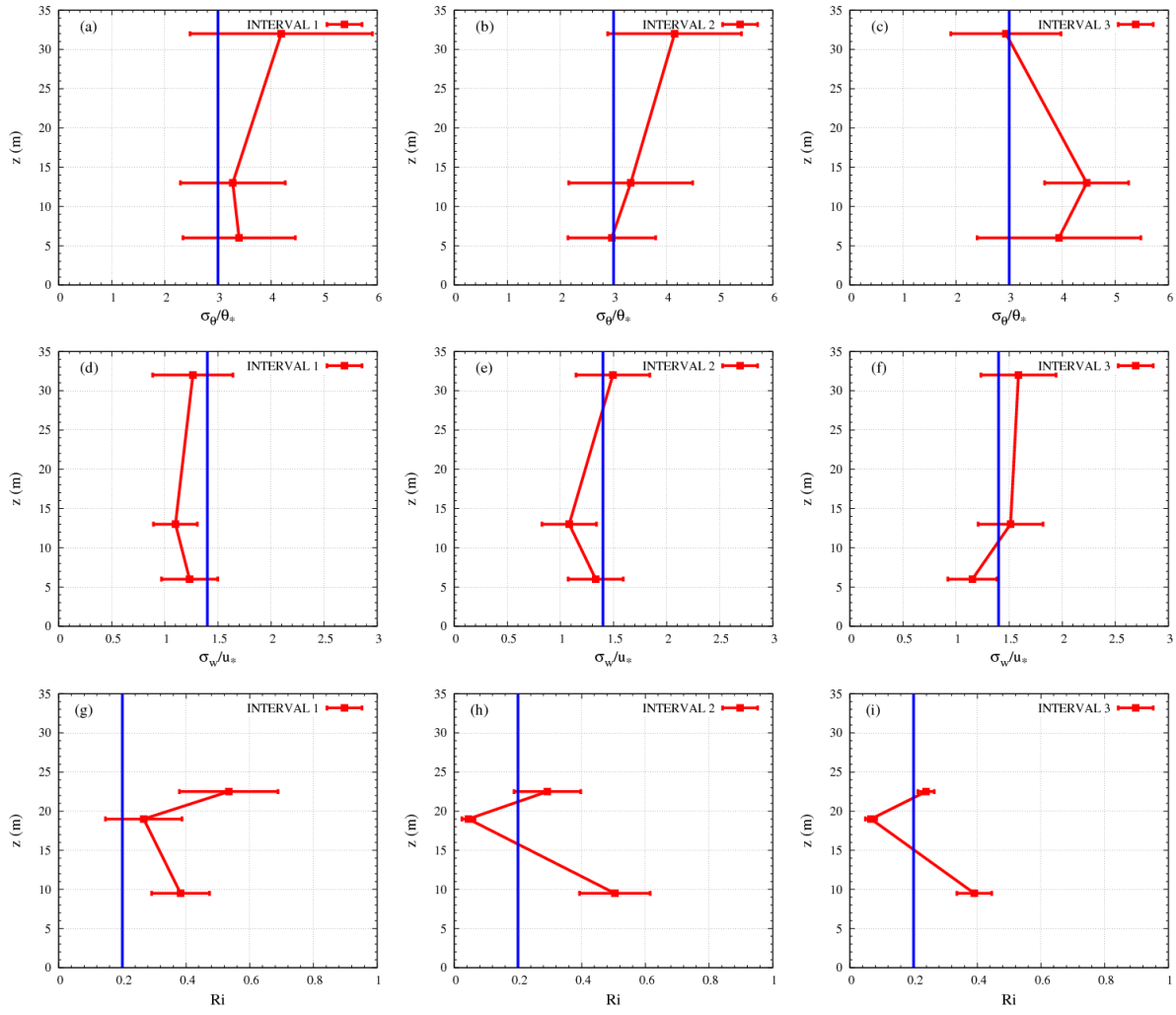

Figure 7. Similarity theory (Nieuwstadt, 1984) applied to each of the night intervals. (a), (b) and (c) σ_θ/θ_*; (d), (e) and (f) the same for σ_w/u_* and (g), (h) and (i) bulk Richardson number. The lines show the trends of each parameter as predicted by Nieuwstadt (1984).

whereas in the higher layers it is below this value. Furthermore, the possibility of turbulence is higher on this level. The upper limit of the SBL can be defined by the inversion height or by the wind maximum. Figure 4b shows the behavior variation in the different intervals. The first period, which is less turbulent in lower layers and is unstable above 13 m, has the maximum of wind (ill defined). It also shows that mixing slightly above the temperature inversion could take place easily as there is an area with wind shear and no significant inhibition from thermal stratification. The second period has the wind maximum below the inversion, which indicates there is a simultaneously production by shear and inhibition by stratification throughout the whole layer, taking different values inside or outside the SL. The last interval is characterized by a nearly perfect superposition of the wind maximum and the inversion which, as in Cuxart and Jiménez (2007), acts as barrier for the mixing through this level. This is broken only sporadically, as indicated by the sodar (Figure 3).

For each interval, Figure 7 shows the profiles of some parameters of the local scaling under stable stability conditions (Nieuwstadt, 1984) for the three levels. Specifically, these are the variances of the fluctuations of vertical speed and of temperature, which are respectively normalized by the parameters u_* -friction velocity-, $\theta_* = \overline{w'\theta'_s}/u_*$ -$\overline{w'\theta'_s}$ is the heat flux on the surface and Λ is the local Monin-Obukhov length-. As shown in Nieuwstadt (1984) or in Garratt (1992, Figure 3.24), in the limit of not too small z/Λ, $\sigma_w/u_* \approx 1.4$, $\sigma_\theta/\theta_* \approx 3$ and $Ri \approx 0.2$.

It could be stressed that Ri takes values which are close or below the theoretical critical value on the second level, which is usually directly above the strong temperature inversion of the SL, indicating that conditions are favorable for the turbulence. This is possibly because the wind there suffers a strong shear when the intensity of the stratification suddenly decreases with height.

Parameter σ_θ/θ_* shows a similar behavior to that predicted by Nieuwstadt for the first two levels and intervals. It indicates that the local scaling can be a good approximation for lower layers but is separated at 32 m, probably because stratification is not very strong at this level. By contrast, for the third interval, which has a higher cooling inversion, this level is also stable and behaves according to the theory. Likewise, there seems to be more turbulence at 13 m than in the other intervals. In contrast to this, for σ_w/u_* values are always close to the theoretical ones, indicating that in all cases vertical speeds are small.

6 Conclusions

Our results show that it is possible to divide the night into three intervals with well differentiated characteristics: the transition between day and night occurs in the first interval, a sustained cooling occurs in the second interval and the third interval is steady. However, this analysis does not aim to generalize or to insist that such patterns are common for similar regimes. It only attempts to assess it as a possible prototypic case.

The first interval, dominated by a surface radiative cooling, allows the decoupling of the residual layer of the surface and the establishment of an oscillation similar to inertial - with a shorter period- which finally generates an LLJ. The second interval has an LLJ where the top of the temperature inversion and the maximum of wind do not coincide. This promotes strong mixing episodes and sustained cooling periods throughout the layer. By contrast, the main characteristic of the third interval is the coincidence between the vertical position and the jet, which acts as a barrier and decouples the upper and lower parts of the jet. Cooling is confined to the SL, with minimum turbulence in this layer.

Local phenomena during the night are significant, and they introduce variability in the time series. In this case, the corresponding PDFs tend to deviate from Gaussianity. More studies of stable nights would be necessary, especially from a climatologic point of view, to confirm if this three-interval pattern could be generalized or if it is merely the influence of local factor in the study place, CIBA. Although a similarity theory under stable stratification conditions is difficult to define, each interval shows different behavior depending on the height where parameters are calculated.

Acknowledgements. We would like to D. Martínez from the UIB for his help in the data processing. Work partially funded by Project CGL2006-12474-C01 of the Spanish Ministry of Science.

References

Chu, C. R., Parlange, M. B., Katul, G. G., and Albertson, J. D., 1996: *Probability density functions of turbulent velocity and temperature in the atmospheric surface layer*, Water Resour Res, **32**, 1681–1688.

Conangla, L. and Cuxart, J., 2006: *On the turbulence at the upper part of the low-level jet: an experimental and numerical study*, Bound-Lay Meteorol, **118**, 379–400.

Conangla, L., Cuxart, J., and Soler, M. R., 2008: *Characterisation of the nocturnal boundary layer at a site in Northern Spain*, Bound-Lay Meteorol, **In press**.

Coulter, R. L. and Doran, J. C., 2002: *Spatial and temporal occurences of intermittent turbulence during CASES-99*, Bound-Lay Meteorol, **105**, 329–349.

Cuxart, J., 2008: *Nocturnal basin Low-Level Jets: An integrated study*, Acta Geophys, **56**, 100–113.

Cuxart, J. and Jiménez, M. A., 2007: *Mixing processes in a nocturnal Low-Level Jet: An LES study*, J Atmos Sci, **64**, 1666–1679.

Cuxart, J., Yagüe, C., Morales, G., Terradellas, E., Orbe, J., Calvo, J., Fernández, A., Soler, M. R., Infante, C., Buenestado, P., Espinalt, A., Joergensen, H. E., Rees, J. M., Vilà, J., Redondo, J. M., Cantalapiedra, I. R., and Conangla, L., 2000: *Stable Atmospheric Boundary-Layer Experiment in Spain (SABLES-98): A report*, Bound-Lay Meteorol, **96**, 337–370.

Cuxart, J., Morales, G., Terradellas, E., and Yagüe, C., 2002: *Study of Coherent Structures and Estimation of the Pressure Transport Terms for the Nocturnal Stable Boundary Layer*, Bound-Lay Meteorol, **105**, 305–328.

Cuxart, J., Jiménez, M. A., and Martínez, D., 2007: *Nocturnal meso-beta basin and katabatic flows on a midlatitude island*, Mon Weather Rev, **135**, 918–932.

Deardorff, J. W. and Willis, G. E., 1985: *Further results from a laboratory model of the convective planetary boundary layer*, Bound-Lay Meteorol, **32**, 205–236.

Garratt, J. R., 1992: The Atmospheric Boundary Layer, Cambridge University Press, Cambridge, 316 pp.

Jiménez, M. A. and Cuxart, J., 2005: *Large-eddy Simulations of the Stable Boundary Layer using the standard Kolmogorov theory: range of applicability*, Bound-Lay Meteorol, **115**, 241–261.

Jiménez, M. A. and Cuxart, J., 2006: *Study of the probability density functions from a Large-Eddy simulation of a stably stratified case*, Bound-Lay Meteorol, **118**, 401–420.

Mahrt, L. and Paumier, J., 1984: *Heat transport in the atmospheric boundary layer*, J Atmos Sci, **41**, 3061–3075.

Mahrt, L., Sun, J., Blumen, W., Delany, T., and Oncley, S., 1998: *Nocturnal Boundarylayer regimes*, Bound-Lay Meteorol, **88**, 255–278.

Monin, A. S. and Yaglom, A. M., 1971: Statistical Fluid Mechanics. Vol. I, The Massachusetts Institute of Technology, 769 pp.

Nieuwstadt, F. T. M., 1984: *The turbulent structure of the stable, nocturnal boundary layer*, J Atmos Sci, **41**, 2202–2216.

Poulos, G. S., Blumen, W., Fritts, D. C., Sun, J. K., Burns, S. P., Nappo, C., Banta, R., Newson, R., Cuxart, J., Terradellas, E., Balsley, B., and Jensen, M., 2002: *CASES-99: A comprehensive investigation of the stable nocturnal boundary layer*, B Am Meteorol Soc, **83**, 555–581.

Smedman, A. S., Bergström, H., and Högström, U., 1995: *Spectra, variances and length scales in a Marine Stable Boundary Layer dominated by a Low-Level Jet*, Bound-Lay Meteorol, **76**, 211–232.

Stull, R. B., 1988: An Introduction to Boundary Layer Meteorology, Kluwer Academic Publishers, Dordretch, 666 pp.

Tennekes, H. and Lumley, J. L., 1982: A First Course in Turbulence, The Massachusetts Institute of Technology, 300 pp.

Yagüe, C., Viana, S., Maqueda, G., and Redondo, J. M., 2006: *Influence of stability on the flux-profile relationships for wind speed and temperature for the stable atmospheric boundary layer*, Nonlinear Proc Geoph, **13**, 185–203.